Small-angle neutron scattering characterization of plastic deformation in amorphous polymers

J. M. Lefebvre and B. Escaig
Structure et propriétés de l'état solide, LA n°234 CNRS Université des Sciences et Techniques 59655 *Villeneuve d'Ascq Cedex, France*

and C. Picot
Centre de Recherches sur les Macromolécules 67083 *Strasbourg Cedex, France*
(*Received* 12 *October* 1981; *revised* 26 *February* 1982)

The direct measurement of coil dimensions resulting from the non-elastic deformation of glassy amorphous polystyrene was undertaken by means of a small-angle neutron scattering technique for various deformation situations. The difference in behaviour between anisotropic glide within a coarse shear band and diffusion-like homogeneous deformation is confirmed on the macromolecular scale.

Keywords Small-angle neutron scattering; glassy polystyrene; plasticity; coil dimensions

INTRODUCTION

The possibility of characterizing the deformation of coils in amorphous polystyrene deformed in the glassy state is examined within the frame of a thermodynamic and kinetic analysis of plasticity. It was established for atactic polystyrene (PS) and poly(methylmethacrylate) (PMMA)[1,2] that, for a given strain rate, two distinct mechanisms in the non-elastic deformation behaviour appear in the temperature range studied, depending on available molecular mobilities:

(i) At lower temperatures, localized heterogeneous glide occurs and may be regarded as analogous to dislocation glide in crystal plasticity against an intrinsic molecular friction.

(ii) At higher temperatures, a new type of molecular mobility, related to secondary relaxations and evidenced by the decrease in elastic modulus, softens this molecular friction; the corresponding behaviour compares well to diffusional plasticity in crystals and strongly depends on the structural history of the material, i.e. on annealing and ageing conditions.

The present paper reports on the direct measurement of chain deformation for both 'glide' and 'diffusional' modes by means of small-angle neutron scattering (SANS). SANS has already proved to be useful in the determination of macromolecular dimensions in bulk, both in the unstretched[3] and in the hot-stretched[4] state.

EXPERIMENTAL

Sample preparation

Cylindrical shaped samples are obtained by compression moulding under vacuum of a mixture of protonated and deuterated polystyrene.

The mixing is done in a chloroform solution; after precipitation in methanol and careful drying, the specimens were moulded under vacuum and subsequently annealed to remove any frozen-in internal stresses.

A summary of the polymer characteristics is given in *Table 1*.

Plastic deformation

Due to strong crazing effects, the mechanical testing of polystyrene in tension, far below the glass transition, is not possible as fracture occurs before the elastic limit has been reached[5]. For this reason, our samples are compressed at constant strain rate in an Instron machine. Deformation conditions in the temperature range $240 < T < 320\,\mathrm{K}$ and strain rate $10^{-6} < \dot{\varepsilon} < 10^{-3}\ \mathrm{s}^{-1}$ are chosen in such a way that the samples should be representative of both modes, i.e. low temperature–high strain rate, or high temperature–low strain rate.

However, since the compression test is not very well suited for further characterization of the deformed samples, the specimen is notched as illustrated in *Figure 1a*; this ensures localization of the plastic deformation within what we call a macroscopic 'shear band' as shown in *Figure 1b*.

This deformation band is extracted from the sample with a high precision diamond saw. No additional deformation is involved as it was checked on the bulk undeformed material. SANS is then done, with the neutron beam along $0x_3$ (see *Figure 1a*).

A first qualitative distinction between the two types of deformation behaviour comes from the birefringence patterns in the plane of the band.

For the glide mode, it is possible to define a unique optical axis throughout the whole band, which coincides with its geometrical axis; whereas in the diffusional case the situation is less simple: although plastic deformation is fairly well localized in the band, the birefringence pattern

0032-3861/82/121751-04$3.00

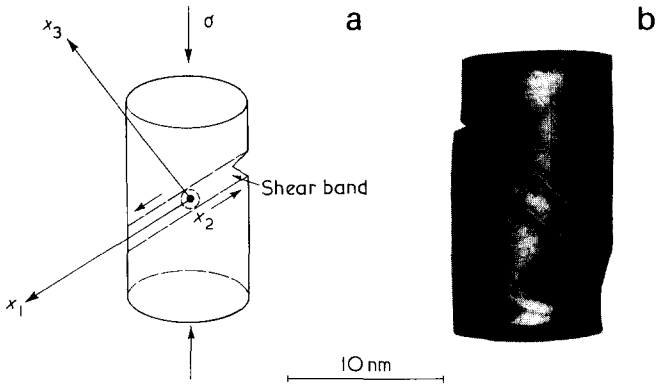

Figure 1 (a) Schematic representation of the sample before compression testing; (b) illustration of the resulting situation, showing the 'shear band'

looks rather random and heterogeneous and no preferred axis is considered. In this case, we refer to the geometrical axis of the band for the sake of comparison with the glide mode.

Neutron small-angle scattering

Experiments were performed on small angle spectrometers D_{11} and D_{17} at the Institut Laue Langevin (Grenoble)[3].

The scattering vectors $q=\frac{4\pi}{\lambda}\sin\frac{\theta}{2}$ were used in this study, lie in the range $5.10^{-3}<q\,\text{Å}^{-1}<2.10^{-2}$ for D_{11} and $10^{-2}<q\,\text{Å}^{-1}<10^{-1}$ for D_{17}.

The scattered intensities were measured for all orientations of the scattering vector in the plane of the band.

The coherent scattering signal from labelled chains is obtained by subtraction of the incoherent scattering background of the matrix evaluated from measurements on purely protonated samples deformed in the same conditions and transmission corrections are also taken into account.

Sample characteristics for the two sets of experiments are summarized in *Table 1*.

In *Table 1*, samples of set 2 have a high PSD content which provides a high coherent scattering signal.

As deduced from incompressibility arguments and verified experimentally by Boué *et al.*[6], the coherent signal of a bulk mixture of identical deuterated and protonated polymers is indeed proportional to $\varphi_D(1-\varphi_D)S(q)$, where φ_D is the number fraction of the labelled species and $S(q)$ the single chain intramolecular scattering function.

Scattering data have been analysed according to the classical anisotropic treatments in the direction parallel to the main axis of the shear band ($q_\parallel$) and transverse ($q_\perp$). Both the Guinier and the intermediate range of scattering distributions have been investigated.

Table 1 Experimental sample characteristics

Samples	Deuteration species fraction φ_D	PSD		PSH matrix	
		M_w	M_w/M_n	M_w	M_w/M_n
Set 1	2%	145 000	1.20	223 000	1.17
Set 2	10%	100 000	1.15	223 000	1.17

RESULTS

Let us consider the two domains of momentum transfer q.

The Guinier range $q\,R_g<1$

The scattering intensity can be written

$$I(q)\sim\left(1-\frac{q^2R_g^2}{3}\right)$$

R_g being the radius of gyration.

Zimm plots $I^{-1}=f(q^2)$ yield values for $R_\parallel$ and $R_\perp$ respectively which are compared with the radius of gyration in the undeformed state R_0; the latter should be related to a z average molecular weight, and values obtained corrected for polydispersity effects, are in good agreement with the R_g molecular weight dependence value $(R_w^2/M_w)^{\frac{1}{2}}\sim 0.28$ already published[3]*.

Illustrations of representative scattering behaviours are given in *Figures 2* and *3* for both deformation modes.

The uncertainty in the R_g determination is to within 3% and the use of the higher labelled species (set 2) improves the counting statistics.

* The measured R_g is also corrected from effects due to differences in molecular weights between the matrix and the labelled species. One has

$$R^2_{g\,\text{app}}=R_g^2\left[1+\frac{\varphi_D\Delta z}{1+(1-\varphi_D)\Delta w}\right]$$

$$\Delta z\sim\Delta w=\frac{M_{wH}}{M_{wD}}-1$$

For detailed analysis, see ref 6.

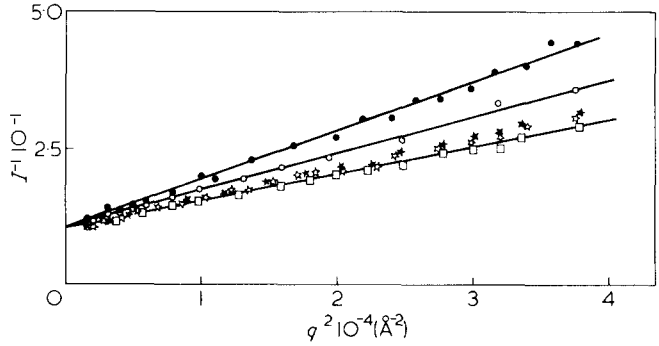

Figure 2 I^{-1} *versus* q^2 plot in the small momentum transfer range — set 1: data identification: (●) $q_\parallel$, (○) $q_\perp$, glide mode; (★) $q_\parallel$, (☆) $q_\perp$, diffusional mode; (□) undeformed

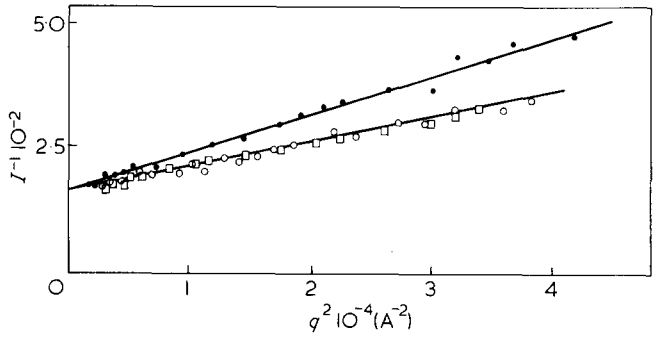

Figure 3 I^{-1} *versus* q^2 plot in the small momentum transfer range — set 2: data identification as for *Figure 2*

Table 2 Longitudinal and transverse coil dimensions

	$R_{\parallel}$ (Å)	$R_{\perp}$ (Å)	R_0 (Å)	Deformation conditions
'Glide' Set 1	148	128	116	$\dot{\epsilon} = 5.10^{-4}\ s^{-1}$ Room temperature
'Diffusional' Set 1'	118	118	116	$\dot{\epsilon} = 5.10^{-6}\ s^{-1}$ Room temperature
'Glide' Set 2	120	97	97	$\dot{\epsilon} = 5.10^{-4}\ s^{-1}$ $T = 250$ K

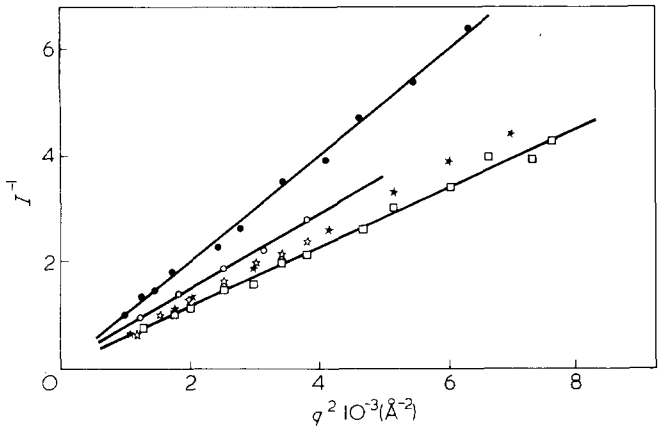

Figure 4 I^{-1} *versus* q^2 plot in the intermediate range – set 1: data identification as for *Figure 2*

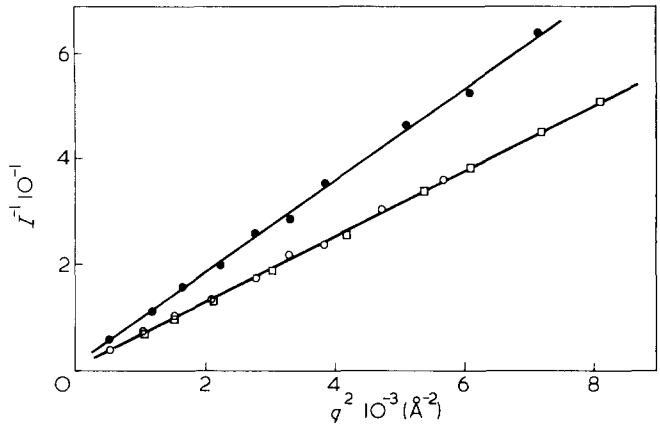

Figure 5 I^{-1} *versus* q^2 plot in the intermediate range – set 2: data identification as for *Figure 2*

A summary of the corresponding longitudinal and transverse coil dimensions is given in *Table 2*.

Before discussing these data, some features are worth noting:

(1) The glide mode reveals marked anisotropy: $R_{\parallel}/R_{\perp} \sim 1.2$. Moreover two situations are occurring: (a) $R_0 = R_{\perp} < R_{\parallel}$ (Set 2), (b) $R_0 < R_{\perp} < R_{\parallel}$ (Set 1).

(2) The diffusional mode behaves in a different way $R_{\parallel} \sim R_{\perp} \sim R_0$ and isointensity contours confirm this isotropy for any axis chosen in the plane of the band.

The intermediate range $R_{\perp}^{-1}$ or $R_{\parallel}^{-1} < q < l^{-1}$

Where l is the statistical unit length. Over this range of scattering vectors, there is no deviation from the Debye linear dependence of the scattered intensity, i.e. $I(q) \sim \frac{K}{q^2}$ for $q_{\parallel}$ or $q_{\perp}$.

The corresponding plots of inverse scattered intensities *versus* q^2 are given in *Figures 4* and *5* for both modes. It appears that the molecular deformation process was constant over the whole range of scales investigated.

DISCUSSION

We firstly concentrate on the anisotropic coil dimensions as observed in the glide mode, in terms of a geometrical analysis of the macroscopic strain in the 'shear band'. Then we will consider the isotropic diffusional mode.

Glide mode: elongated coils

The following analysis is made within the framework of the linear theory of small strains.

Figure 6a provides a schematic representation of the

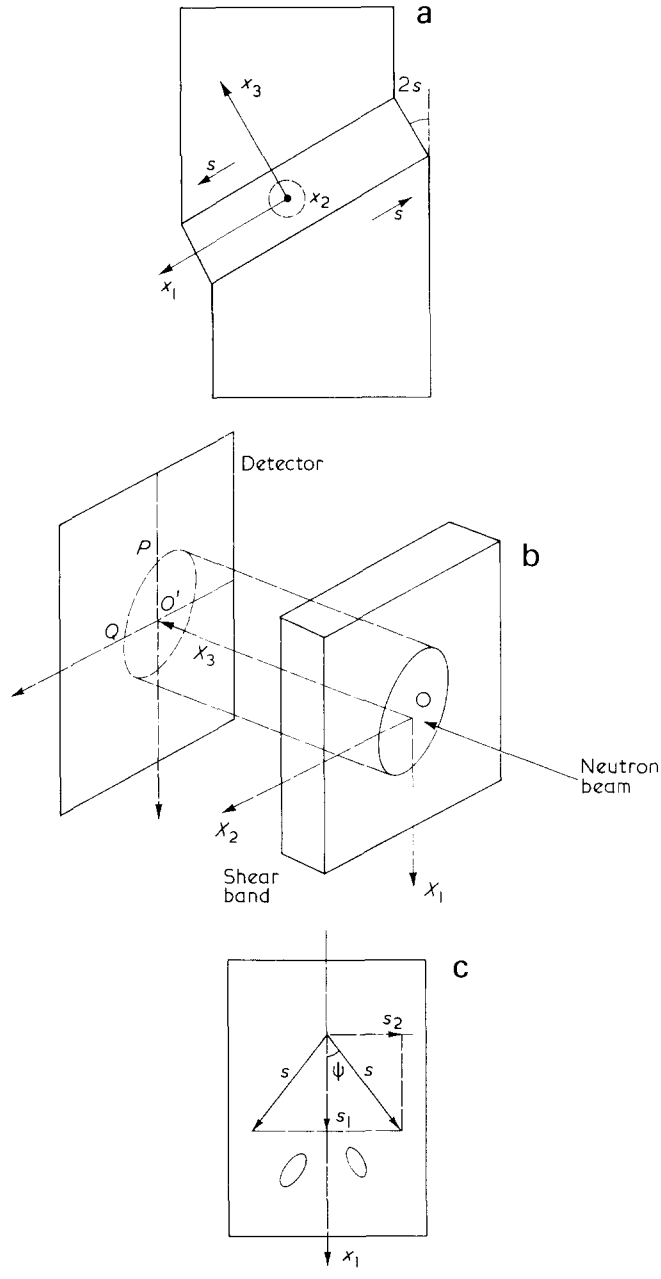

Figure 6 Geometrical analysis of coil elongation (a) the 'shear band' viewed within the sample; (b) projection of a sheared sphere on plane $(\hat{x}_1, x_2)$; (c) shear band viewed along $\hat{x}_3$ in the case $R_0 < R_{\perp} < R_{\parallel}$

deformed sample. Let $\hat{x}_1$, $\hat{x}_2$, $\hat{x}_3$ be unit vectors of the cartesian coordinates system attached to the shear band. The strain is a measure of the shearing angle $2S$.

(i) Being given the strain tensor $\bar{\bar{\varepsilon}}=\begin{pmatrix}0 & 0 & S\\ 0 & 0 & 0\\ S & 0 & 0\end{pmatrix}$, the ultimate shape of a sphere φ at the origin of the coordinates is unique and only depends on S.

A simple choice for the particle displacement field is for example $u(r)=\hat{x}_1.2Sx_3$

Thus $O\vec{M}(x_1, x_2, x_3)$ where $M\varepsilon\varphi$ becomes

$$O\vec{M}'=O\vec{M}+\vec{u},\ O\vec{M}'(x_1', x_2', x_3')$$

It is fairly straightforward to show that the sheared sphere has become an ellipsoid, the projection of which is observed on the screen parallel to the plane of the band $(\hat{x}_1, \hat{x}_2)$. This leads, according to the definitions of *Figure 6b*, to values for apparent radii along $\hat{x}_1$ and $\hat{x}_2$ respectively as

$$O'P=R_{\parallel}=R_0\sqrt{1+4S^2}$$

$$O'Q=R_{\perp}=R_0$$

This accounts for the situation (a) $R_0=R_{\perp}<R_{\parallel}$ (Set 2) discussed earlier.

(ii) If one combines the preceding displacement field with rotations of the ellipsoids around $\hat{x}_3$ in the plane of the band symmetrically distributed with respect to $\hat{x}_1$, one obtains the situation roughly illustrated in *Figure 6c*. Such considerations have to account for two experimental facts linked with the case (b) $R_0<R_{\perp}<R_{\parallel}$ (Set 1) discussed earlier. These are (1) $\hat{x}_1$ is the optical axis of the band; (2) lateral overflowing of matter is observed on the sample (i.e. the final transverse dimension of the 'shear band' is wider than the radius of the initial cylinder).

A more realistic description in terms of the particle displacement field is then to take:

$$u(r)=\hat{x}_1 2S_1x_3+\hat{x}_2.2S_2x_3$$

yielding

$$\bar{\bar{\varepsilon}}=\begin{pmatrix}0 & 0 & S_1\\ 0 & 0 & S_2\\ S_1 & S_2 & 0\end{pmatrix}$$

Adopting the same mathematical procedure as in (i) the apparent radii along $\hat{x}_1$ and $\hat{x}_2$ are obtained

$$O'P=R_{\parallel}=R_0\sqrt{1+4S_1^2}$$

$$O'Q=R_{\perp}=R_0\sqrt{1+4S_2^2}$$

in agreement with situation (b) above.

(iii) This simple description allows us to explain the measured anisotropic coil dimensions observed in the 'glide mode' in terms of simple shear occurring in the plane of the band, either parallel to the longitudinal axis $\hat{x}_1$ ($R_0=R_{\perp}<R_{\parallel}$) or at some angle $\pm\psi$ from $\hat{x}_1$ and symetrically apart ($R_0<R_{\perp}<R_{\parallel}$) (see *Figure 6c*).

Applying this to the measured radii, gives:

(a) $R_{\parallel}=120$ Å, $R_{\perp}=97$ Å $=R_0$, $S=0.37$ and the shearing angle is $\gamma\sim 42°$.

(b) $R_{\parallel}=148$ Å, $R_{\perp}=128$ Å, $R_0=116$ Å.

$S_1=0.39$ and $S_2=0.23$ which yields, referring to *Figure 6c*,

$$S=\sqrt{S_1^2+S_2^2}=0.45 \text{ and } \psi\simeq 30°.$$

The shearing angle is then $\Psi\simeq 50°$.

The occurrence of either of these situations is purely mechanistic; it clearly depends on the way in which deformation initiates at the notch and has no molecular origin.

Diffusional mode: undeformed coils

The behaviour of the high temperature–low strain-rate mode, however, confirms our previous kinetic analysis of plasticity based on purely mechanical investigations in amorphous polymers.

Deformation should then proceed by chain intercalation at the level of a few monomer units, resulting in rather random chain orientation. The molecular mobilities associated with secondary relaxations may account for this diffusional behaviour. Moreover this diffusive character might be responsible for a certain averaging of the deformation directions within the 'shear band'.

Further work is in progress on this mode, together with optical measurements (birefringence and fluorescence polarization) in the band.

ACKNOWLEDGEMENTS

This work was made possible by beam time allocation on D_{11} and D_{17} spectrometers at the Institut Laue Langevin, Grenoble.

We wish to thank R. Duplessix and M. Rawiso for their help during the course of these measurements.

REFERENCES

1 Cavrot, J. P., Haussy, J., Lefebvre, J. M. and Escaig, B. *Mater. Sci. Eng.* 1978, **36**, 95
2 Haussy, J., Cavrot, J. P., Escaig, B. and Lefebvre, J. M. *J. Polym. Sci., Polym. Phys. Edn.* 1980, **18**, 311
3 Cotton, J. P. *et al. Macromolecules* 1974, **7**, 863
4 Picot, C. *et al. Macromolecules* 1977, **10**, 436
5 Hoare, J. and Hull, D. *J. Mater. Sci.* 1975, **10**, 1861
6 Boué, F., Nierlich, M. and Leibler, L. *Polymer* 1982, **23**, 29